SLAC-PUB-14440

COUPLER STUDIES for PBG FIBER ACCELERATORS*

J. England, C. Ng, R. Noble, J. Spencer#, Z. Wu and D. Xu, SLAC, Menlo Park, CA 94025, U.S.A.

Abstract

Photonic band gap (PBG) fiber with hollow core defects are being designed and fabricated for use as laser driven accelerators because they can provide gradients of several GeV/m for picosecond pulse lengths. We expect to produce fiber down to λ=1.5-2.0 μm wavelengths but still lack a viable means for efficient coupling of laser power into such structures due to the very different character of the TM-like modes from those used in the telecom field and the fact that the defect must function as both a longitudinal waveguide for the accelerating field and a transport channel for the particles. We discuss the status of our work in pursuing both end and side coupling. For both options, the symmetry of these crystals leads to significant differences with the telecom field. Side coupling provides more options and appears to be preferred. Our goals are to test gradients, mode content and coupling efficiencies on the NLCTA at SLAC.

INTRODUCTION

While there are many potential types of fiber based on very different fabrication methods and materials we will concentrate on 2D axisymmetric glass with hexagonal symmetry but will discuss several different geometries including 2D and 3D planar structures. Since all of these can be fabricated using modern techniques with a variety of dielectric materials they are expected to have desirable optical and radiation hardness properties. Thus, we expect a new generation of very high gradient accelerators that extends the Livingston-Panofsky chart of exponential growth in energy vs. time at greatly reduced costs. For illustration, Fig.1 shows a simulation of our first engineered fiber with an accelerating mode expected near 7.3 μm that is now ready to test on the NLCTA.

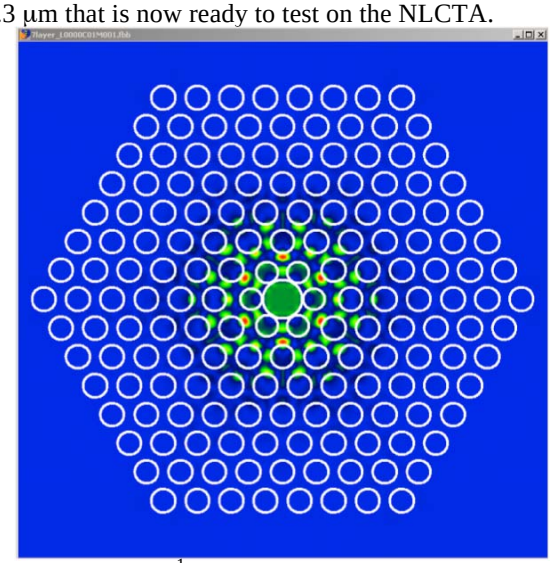

Figure 1: CUDOS[1] simulation of fiber from Incom, Inc[2].

*Work supported by DOE contract DE-AC02-76SF00515.

#jus@slac.stanford.edu

In this example, one sees the uniform longitudinal accelerating field in the central defect as first shown by Lin[3] together with a hexagonal array of surrounding hot spots. Contrary to what one expects from the telecom field, Ng et al. have shown[4] that the ideal end-coupling scheme for this structure appears as shown in Fig. 2 with a six-fold array of laser spots focused inside the end of the fiber. While convenient for an on-axis particle beam, this is inconvenient for the laser drive field as well as the tolerances it places on the end cleave of the fiber.

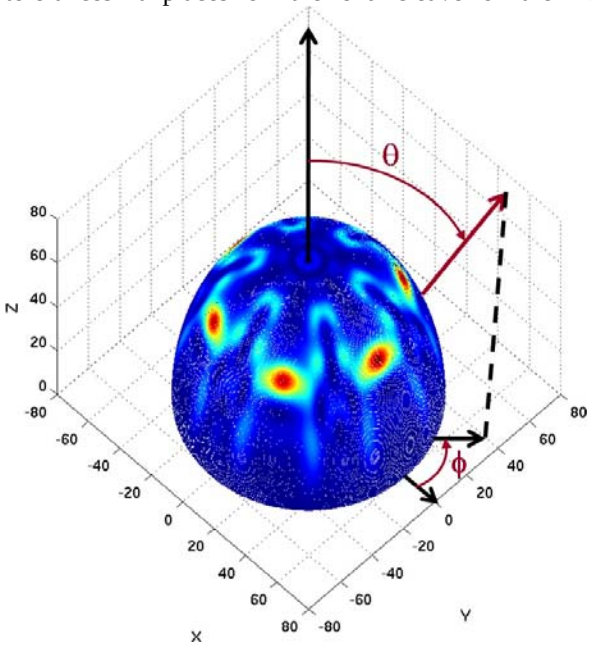

Figure 2: Poynting flux on the surface of a hemisphere of radius 80λ whose z-axis is along the fiber axis normal to the exit of the fiber. The rainbow color scheme represents the magnitude with red-blue the maximum and minimum.

The importance of the crystal symmetry is clearly shown so that one might expect side coupling to reflect a similar pattern which we find that it does unless the hexagonal symmetry is perturbed sufficiently. This can be done in several ways and will be discussed further below.

DIFFERENT FIBER TYPES

Comparing design goals for the telecom and accelerator fields shows that they are almost dual to one another based on their emphasis on either core or surface modes. While one uses TE-like modes, the other TM-like and while one can use solid core the other needs hollow core resulting in surprisingly little cross fertilization. Thus, due to the comparative simplicity of the telecom problem and its obvious commercial aspect that field has made great progress. The other is nearly unexplored so we begin by discussing the dimensionality of the competing structures.

The basic symmetry of the lattice follows from the shape of the central defect which is typically circular but can be any of a number of shapes esp. square depending on the demands of the application and the capillary sizes and shapes that are available. While it is easier to manufacture the circular defects such as shown in Fig. 1, it is possible to make almost any shape and still produce acceptable modes. Both square and circular defects can produce very homogeneous beams across their apertures as shown in Fig. 1 but because many semiconductors such as ccd's and laser diodes have rectangular working areas (for some unknown reason), rectangular defects may have greater capture efficiencies. We will discuss several examples and their possible advantages next.

2D-Structures

The 2D structure in Fig. 1 has a refractive index that is a function of the transverse dimensions (x,y) where the particle and laser beams propagate along z considered infinite but is actually piecewise perturbed e.g. by coupler disks. The ratio of defect radius R to lattice capillary period is R/a=0.59 with the TM-like speed-of-light (SOL) mode at 7.3 μm. The accelerating gradient to maximum E field in the glass is G/E_{max}=0.4 yielding gradients well in excess of a GeV/m for many materials. For end-coupling into this structure [4], one propagates the basic accelerating mode down the fiber and observes the far-field radiation pattern from the end to determine whether one can make a reasonably efficient time-reversed facsimile as in Fig. 2 where we estimate η_{EC}~0.80[4]. An equivalent approach for side coupling into the structure in Fig. 1 is given in Fig. 3A while Fig. 3B shows how to enhance that result by removing one ring. We observe the same far-field symmetry in all cases with only minor changes to the accelerating mode.

It is possible to reduce the number of laser beams and improve efficiency by breaking the hexagonal symmetry (or other symmetries) by adding defects. One example, the simplest, is to add a line of defects between opposing vertices and increase the number of rings appropriately in Fig. 1. With three defects across the median plane (Fig. 4) the radiation pattern reduces from six to two so that only two laser spots are required to drive three defects. Further, by removing either of the new defects, only one laser spot is required to drive two defects.

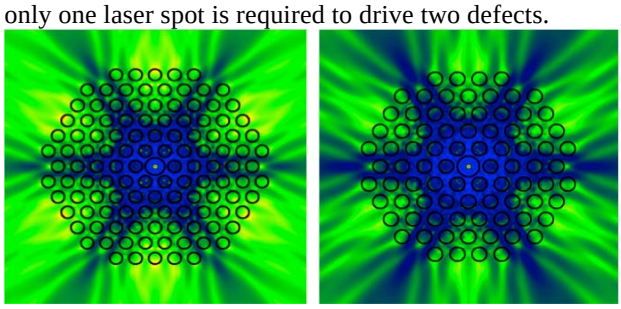

Figure 3: (A) One sees a more directed, enhanced radiation pattern from removing six vertex capillaries from Fig. 1. Blue is the highest value in these plots of Log[S_r]. (B) Removing a ring further enhances the radiation with minimal effects on the accelerating mode.

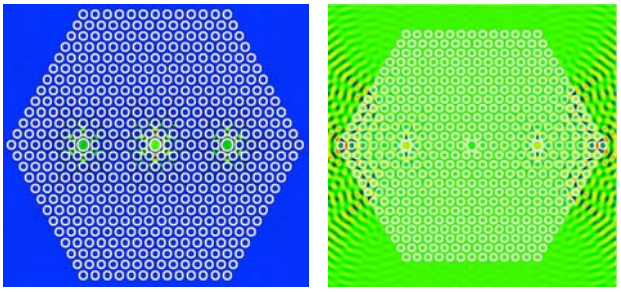

Figure 4: (A) Multi-defect mode with local distributions analogous to Fig. 1. (B) Radiative field component Re[E_z] dominated by the constructive interference between the radiative losses from the three defects excited with the same longitudinal accelerating mode.

Alternative schemes for end and side coupling free space laser modes into 2D structures are also of interest when efficient i.e. they occur within a few wavelengths.

As shown in Fig. 5(a), the incident laser mode enters the simulation region through the boundary on the left and propagates through a region of vacuum to the right (positive z direction). The vacuum-fiber interface occurs at the z=0 plane and extends for 20 wavelengths (λ = 2 μm) before terminating on an absorbing boundary condition (ABC). The input power P_{in} of the incident radiation field scales with the focal RMS waist size w_0 and electric field amplitude E_0 as $P_{in} \propto |E0|^2 w_0^2$. Coupling to the accelerating mode was optimized by varying w_0 and the longitudinal position of the focal point. The maximum coupling was found to occur for a nominal focus one wavelength inside the fiber and a waist size $w0 \leq \lambda/4$. From the plot of forward power P_{FWD} coupled to the mode in Fig. 5(b), we see that after a formation length of approximately 5 wavelengths, the fraction of forward power in the mode decreases to 16.5% over the full 20 wavelengths (power reflected into the negative z direction is effectively zero). This decrease is accompanied by a decrease in overall power in the waveguide by 55% over the same propagation distance due to shedding of unconfined radiation modes, so the fraction of power coupled into the accelerating mode constitutes 38% of the total power propagating in the waveguide at the downstream end of the simulation volume. The remaining 62% of the propagating power presumably belongs to various lossy (unconfined) modes which will tend to leak out of the fiber over the course of several hundred wavelengths of propagation distance.

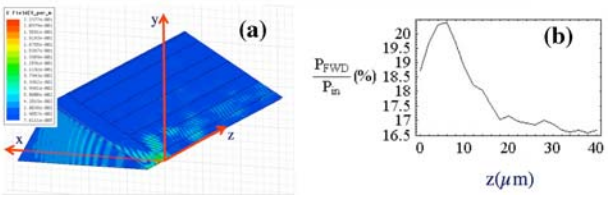

Figure 5: HFSS simulation geometry (a) for a Gaussian TEM_{01}* like laser mode incident on the PBG fiber in the +z direction, and (b) calculated fractional forward power in the desired mode as a function of z.

Before leaving this section we show an actual structure that was fabricated to specifications that should have given a good accelerating mode using available glass capillary in Fig. 6. Simulations of the as-built structure shown above in Fig. 1 appear to bear this out. The defect shown is just one of many that is embedded in an array of hexagonal structures such as shown in the previous figures.

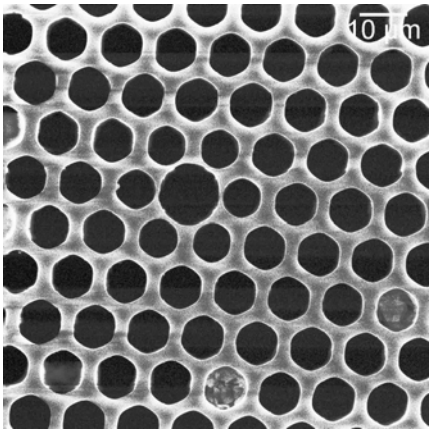

Figure 6: A typical SEM picture of the structure fabricated by Incom, Inc[2] and simulated above in Fig.1. The two occlusions at the lower right are from polishing compound.

3D-Structures

Coupling photons into the accelerating mode in 3D woodpile defect structures can follow the same criterion: energy needs to be coupled to the hot spots surrounding the defect channel. Figure 7 depicts the accelerating mode in the woodpile waveguide, with four hot spots providing portals into the defect. Unlike 2D fibers, 3D PBGs may confine EM waves omni-directionally, allowing direct air channels to be opened in the lattice to send energy in e.g. a T-junction side coupler similar to those constructed by metallic RF waveguides should be realizable in 3D PBG structures.

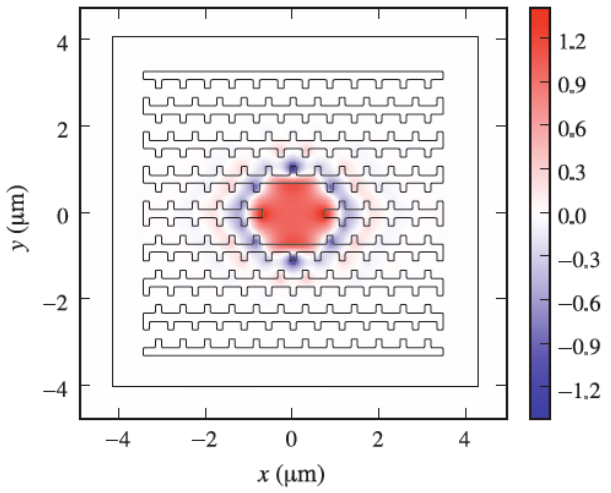

Figure 7: TM mode in the woodpile waveguide for electron acceleration. One sees that the strong central field extends into the lattice at top and bottom and on the sides.

Previously, Cowan[5] proposed the T-junction coupling design shown in Fig. 8. The coupling was optimized in a reversed way. The fundamental accelerating mode, solved from eigenmode simulations, is launched in the guide towards the T-junction. The extrusion lengths of several silicon rods at the coupling corner, as can be seen in Fig. 8, were adjusted individually to maximize the power coupled into the coupling guide. Via numerous parametric simulations, it has been found that Rod Y_2 and Y_3 most significantly affect the coupling. An Y_2 and Y_3 extrusion of $0.1a$ and $0.5a$, respectively, yields an optimized coupling efficiency of over 95%, a being the lattice constant. Granted the fields in the coupling guide as the input, time-reversal theorem then guarantees that over 95% total power would be coupled into the right mode in the accelerating guide. An asymmetric rod setup asides the $x=0$ plane at the T-junction could selectively couple the power into the forward direction electrons get accelerated towards.

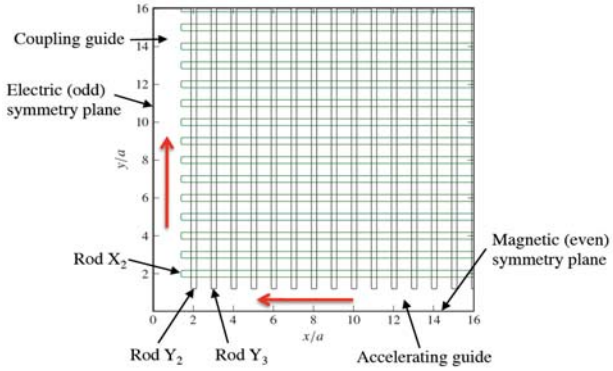

Figure 8: Schematic of the T-junction between woodpile accelerating guide and coupling guide. Several silicon rods are tweaked to optimize the power coupling.

ACKNOWLEDGEMENTS

We would like to thank our collaborators at Incom, Inc. for their many contributions to this work and especially DCB, MAD, MJM, JAK, JMR, RJM and DWS to mention only a few. Also, Patrick Lui at SLAC who has helped in so many ways to make this collaboration a success as well as Eric Colby for useful discussions and use of his Matlab code for far-field calculations shown in Fig. 2 and also Ben Cowan for all his past and present work on 3D structures.

REFERENCES

[1]CUDOS MOF Utilities for micro-structured optical fibres, Boris Kuhlmey, Univ. of Sydney, Australia, http://www.physics.usyd.edu.au/cudos/mofsoftware

[2]Incom Inc, 294 Southbridge Road, Charlton, MA01507

[3]X. E. Lin, Phys. Rev. ST Acc. Beams 4, 051301 (2001)

[4]C.-K. Ng et al., Phys. Rev. ST Acc. Beams 13, 051301 (2010)

[5]Benjamin M. Cowan, Phys. Rev. ST Acc. Beams 11, 011301 (2008)